RSC Advances

PAPER

View Article Online
View Journal | View Issue

Cite this: *RSC Adv.*, 2020, **10**, 10959

Sustainable oxidation of cyclohexane catalyzed by a $VO(acac)_2$-oxalic acid tandem: the electrochemical motive of the process efficiency†

Alexander Pokutsa, *[a] Pawel Bloniarz,[c] Orest Fliunt,[b] Yuliya Kubaj,[a] Andriy Zaborovskyi[a] and Tomasz Paczeŝniak[c]

Received 16th January 2020
Accepted 27th February 2020

DOI: 10.1039/d0ra00495b

rsc.li/rsc-advances

Cyclohexane oxidation by H_2O_2 to cyclohexanol, cyclohexanone, and cyclohexylhydroperoxide under mild (40 °C, 1 atm) conditions is significantly enhanced in the system composed of $VO(acac)_2$ (starting catalyst) and small additives of oxalic acid (process promoter). In corroboration of this, several times higher yield of the desired products was obtained compared to that obtained in the acid-free process. The revealed advantage was addressed to elevate the electrical conductance *G* (or *vice versa*, decreasing the resistance, 1/*G*) of the reaction medium. On the other hand, the content of oxalic acid (20–30 mM) was compulsory to optimize the process parameters. The last value of concentration affords, besides the lowest 1/*G*, the utmost impact on pH, redox potential, and current–voltage relationships. Exceeding this level leads to an increase in 1/*G* of the reaction solution, ceases the impact on pH, ORP, and CV profiles, and is detrimental for the product yield. The putative mechanism of the revealed effects has been envisaged.

1. Introduction

Cyclohexane (CyH) liquid phase homogeneous oxidation remains the key process of cyclohexanol (COL), cyclohexanone (CON), and cyclohexylhydroperoxide (CHHP) manufacturing. Because of the exceptionally high C–H BDE (about 100 kcal mol),[1] the process is carried out at increased temperature (160–180 °C) and air pressure (13–15 atm) in presence of Co(II) catalysts. Despite such severe conditions, the commercialized process is characterized by very low (4–6%) substrate conversion and moderate (75–80%) selectivity by the COL + CON mixture.[2] The higher level of conversion is curbed by the free-radical mechanism responsible for the side reactions of over-oxidation that are particularly detrimental to the selectivity.[3]

Given the commercial importance of these products in terms of the global needs in artificial fibers (nylon 6, nylon 6,6) and energy-efficient processes, any advance in this area would be of high commercial impact. On the other hand, the inactive C–H bonds make C_6H_{12} a proper candidate for the ultimate probing of the activity of designed catalysts that is of particular interest in fundamental chemistry. Altogether, such knowledge could render the elaboration of protocols that can potentially intensify the oxidative transformation of others substrates of practical interest.

To date, numerous attempts related to the synthesis of metallocomplex catalysts constitute d-elements cations and various ligands.[4,5] The alternative ways embrace the elaboration of relevant reaction medium[6] as well as systems that are able to mimic the work of metalloenzymes (*e.g.*, methane mono-oxygenase).[7,13] The benefits of such strategy sometimes, but not always, embrace the C–H bond activation and, as a result, enhance the process effectiveness.[8] However, the commercial implementation of such technologies still lack acceptable productivity/cost ratio.

The versatile and inexpensive methods of C–H bond functionalization were found to use Schiff bases, alkanolamines, phenolamines,[9] pyridine-2-carboxylic acid (PCA) accompanied with ketone (butanedione),[10] and *N*-hydroxyphthalimide (NHPI),[11] which noticeably increase the oxidation efficiency. Inspired by the cited studies, we scrutinized the activation abilities of glyoxal as a simpler analog of butanedione where CH_3-groups are substituted by H-atoms.[12] On the other hand, since oxalic acid (OxalH) was the product of glyoxal oxidation,[14] its potential impact on the studied process was also investigated. As revealed, the yield of the products can be sufficiently improved by application of the $VO(acac)_2$ catalyst together with OxalH.[12] The mechanism of this phenomenon embraces the *in situ* generation of $VO(oxalate)_2$, which can consequently interact with H_2O_2. Among others, it leads to the species composed of the $VO(\eta^2\text{-}O)_2$ core, which manifests itself as a selective (contrary to the free radicals) and active oxygenation agent.[14]

[a]*Department of Physical Chemistry of Fossil Fuels, Institute of Physical Organic Chemistry and Chemistry of Coal NAS of Ukraine, Naukova Str., 3A, Lviv 79060, Ukraine. E-mail: apokutsa@ukr.net; Fax: +38 032 263 51 74; Tel: +38 032 263 51 74*

[b]*Ivan Franko National University of Lviv, Faculty of Electronics and Computer Technologies, Dragomanov Str., 50, Lviv, 79005, Ukraine. E-mail: orf@online.ua*

[c]*Rzeszow University of Technology, P. O. Box 85, 35-959 Rzeszow, Poland. E-mail: bloniarz@prz.edu.pl*

† Electronic supplementary information (ESI) available. See DOI: 10.1039/d0ra00495b

Most previously undertaken studies involve traditional chemical approaches to assess the enhancing effect of catalysts and additives on the process efficiency. On the other hand, the literature that elucidates the impact of electrochemical parameters on the process, apart from cyclic voltammetry (CV) studies, remains rather short and covers pure solvents only.[15,16] In view of this, we decided to examine the ability of reaction medium constituents (*e.g.*, catalyst, mediator, and oxidant) to modify the electrochemical properties other than the well-studied pH or current–voltage relationships. Working on this problem established that the effectiveness of cyclohexane oxidation is dependent on the relative dielectric permittivity of the reaction solution,[17] whilst the electric conductance G (or *vice versa* electric resistance, $1/G$) alteration accompanied by electric current–potential and pH dependencies have not been investigated yet although they may also affect the oxidation process.

In order to study the influence of selected electrochemical parameters on the process yield and mechanism, catalytic tests were undertaken together with impedance, CV, and pH measurements. The outcome of such an approach is reported herein.

2. Experimental

2.1 Materials

A commercial aqueous solution of hydrogen peroxide (35 wt%, Fluka) was concentrated to 70 wt% by vacuum distillation at 45 °C/10 mm Hg (caution: risk of explosion. All glassware has to be thoroughly rinsed with distilled water to remove traces of any heavy metals). As the purity of commercial $VO(acac)_2$ (Aldrich) is *ca.* 95%, it was dissolved in MeCN to obtain a saturated solution, which was then filtered through a micro-porous paper filter. The filtrate was evaporated at 40 °C under reduced pressure and the resulting solid was dried under vacuum at 20 °C for 48 h, leading to tiny dark-green (0.5–1.0 mm) crystals, which were used in the oxidation experiments. Cyclohexane, acetonitrile, triphenylphosphine (Ph_3P), and tetra-*n*-butyl ammonium perchlorate (Aldrich) were analytical grade and used as received.

2.2 Analytical techniques

The set of selected analytical methods, namely, gas–liquid chromatography (GLC), impedance, CV, pH, and iodometry, have emerged as non-invasive tools that provide evidences concerning the process mechanism.

The low-frequency complex dielectric spectra of the studied solutions can be well fitted with the equivalent electrical circuit containing dispersive power capacitor (B, n) and equivalent electrical R_vC_V circuit in series (the principal electrical Scheme S1 of this device and relevant explanations are given in the ESI†). Fitting the low-frequency dielectric spectra allows to obtain the true non-dispersive values of volume conductance/resistance and relative dielectric constant of the solutions under study that is not possible by usual direct current techniques. Solutions conductance G equals $1/R_v$. The detailed description of application GLC, impedance, CV, pH, and iodometric methods has been provided earlier.[14,17]

2.3 Cyclohexane oxidation

The experiments were carried out in 25 mL round bottom glass flasks equipped with a reflux condenser and a magnetic stirrer. In a typical experiment, cyclohexane (3.36 g, 40 mmol) was dissolved in MeCN (15 mL) containing $VO(acac)_2$ (0.0032 g, 0.012 mmol) and oxalic acid (0.038 g, 0.3 mmol). The mixture was preheated at 40 °C for 5 min before the addition of H_2O_2 (1.34 g, 40 mmol). This moment corresponds to the beginning of the oxidation reaction. Usually, the reaction was carried out for 5 h under atmospheric pressure and vigorous stirring. The reaction mixture was sampled in regular intervals and analyzed by iodometry and GLC (Hewlett-Packard 5890, Series II, flame-ionization detector, capillary column 30 m × 0.25 mm, immobile phase HP-Innowax) and LKhM-80 (flame-ionization detector, packed column 3 m × 3 mm, immobile phase OV-17 on Chromaton N-AW, internal standard 1-heptanol. More details concerning this analysis can be found in previous works.[14,17]).

3. Results and discussion

3.1 Steering the oxidation process by oxalic acid additives

3.1.1 Impact of oxalic acid on the yield and product distribution. $VO(acac)_2$ taken at <0.6 mM in the absence of OxalH resulted neither in the aimed product yield nor led to H_2O_2 consumption (entry 1, Table 1). The total yield of COL + CON + CHHP as well as ΔH_2O_2 value become detectable starting from the concentration of $VO(acac)_2 \geq 0.6$ mM (entry 2, Table 1). On the other hand, in the presence of OxalH, a very tiny amount of $VO(acac)_2$ (0.06 mM) increased the productivity by ~45 times compared to the conditions without OxalH (Table 1, Fig. 1). Supplementing the initial reaction solution with oxalic acid affects, apart from the total yield elevating, the product distribution. The last value was not constant and varied in the course of process evolution due to $C_6H_{11}OOH$ decomposition to $C_6H_{11}OH$ and $C_6H_{10}(O)$ (Fig. S1a–d†). For instance, the discussed COL/CON/CHHP ratio is altered from 7/12/1 (acid-free process, entry 2) to 1/8/90 when oxalic acid was taken in a comparable $VO(acac)_2$ amount (entry 3). Further increasing the OxalH content diminished the relative amount of cyclohexylhydroperoxide, resulting in the yield of these products in roughly 4/1/4 ratio (compare entry 3 with 4, 5, and 6). The last results correspond to the kinetics of products accumulation (compare the plots a, d with b, c, Fig. S1†). Usually the product distribution value was seconded (among others) by the rate of CHHP generation/decomposition. For example, in the process guided by a minute amount of OxalH (≈1 mM, *i.e.* ≈0.05 mM of H^+), the equilibrium of reaction (1a) (Scheme 1) is shifted to the right side, thus benefiting the homolytic cleavage of H_2O_2. Accordingly, the yield of CHHP as pure radical-dependent product became relatively higher contrary to the one obtained in acid-free oxidation. However, higher (>40 mM) OxalH concentration caused a significant decrease in the solution pH, which benefits the non-radical cleavage of initial H_2O_2, thus lowering the yield of CHHP (section below).

The highly reactive $RO^{\bullet}$ radicals as well as (although to a lesser degree) $ROO^{\bullet}$ radicals trigger the cascade of free radical transformations of the substrate to CHHP.[14] As soon as the last

Table 1 The yield of products and catalyst turnover number (TON) value dependent on the reaction mixture composition[a]

				Selectivity, mol%					
Entry	$VO(acac)_2 \times 10^3$, M	OxalH $\times 10^3$, M	ΔCyH%	COL	CON	CHHP	TON	ΔH_2O_2[b], %	$Eff_{H_2O_2}$[c], %
1	0.06	—	<0.1	—	—	—	—	≈1	n/r
2	0.6	—	1.2	33	62	5	23	48	4.2
3	0.6	1.0	1.7	1	8	91	51	52	6.5
4	0.6	15	5.3	48	7	45	169	96	11.0
5	0.6	50	7.6	43	13	44	253	90	16.9
6	0.6	150	5.2	47	10	43	173	80	13.0
7	0.06	50	5.1	23	25	43	1516	25	42.4
8[d]	0.06	15	30	22	44	34	944	34	17.6
9[e]	0.6	—	0.6	1	2	97	18	19	6.5
10[e]	0.6	15	<0.1	Trace	Trace	Trace	<1	10	n/r
11[e]	0.6	1.0	0.1	1	1	98	3	15	1.5

[a] $[CyH]_0 = [H_2O_2]_0 = 1.8$ M; $[VO(acac)_2]_0 = 0.06 \times 10^{-3}$ M. MeCN, 40 °C, 5 h. [b] Amount of H_2O_2 consumed. [c] $Eff_{H_2O_2}$ is the ratio of stoichiometric (due to the product yield) amount of H_2O_2 divided by the H_2O_2 consumed (considering that from 2 g mol of H_2O_2, 1 g atom of O_2 can be produced; thus, up to 50% of H_2O_2 taken can be used for the purpose of oxidation). [d] $[CyH]_0 = 0.18$ M. [e] $Co(acac)_2$ was used instead of $VO(acac)_2$. ΔCyH (substrate conversion) coincides with the product yield according to the almost 100% process selectivity (besides COL, CON, and CHHP, any products, for *e.g.*, adipic acid or caprolactam were not detected). N/r – not reckoned.

product emerges, the –O–O– bonds can be easily broken by the assistance of cations or free radicals (Scheme 1, reaction (2b); Scheme 2). Given the Table 1 and Fig. S1† data, both COL and CHHP were discerned as two principal products whereas CON was the minor one. Despite the fact that the last product of radical-induced CHHP decay should be predominant (route b and intra-molecular rearrangement route c, Scheme 2), in reality, it was COL (Table 1, Fig. S1†). Hence, one can admit that the homolysis of CHHP prevails over its radical-induced counterpart. The relative decrease in the CHHP yield was detected once the concentration of OxalH in the initial mixture started to increase (runs 4–6, Table 1). The last result could be attributed to the heterolytic decay of peroxides, which occurs preferably at low pH (reaction (3b) and the section below). Such features significantly reduce CHHP production. Similarly, a decrease in the initial concentration of C_6H_{12} decreases the yield of $C_6H_{11}OOH$ and leads to the product ratio of 1/2/1.5 in spite of the presence of OxalH (compare entry 6 with 8 of Table 1 and Fig. S1b with S1c†). The last feature corresponds to the much lower rate of radical propagation step stipulated by the diminished substrate content. In contrast, high catalyst concentration increases the yield of CHHP, which indicates the ubiquity of free radical transformation of the substrate (compare Fig. S1d with S1a–c†). Therefore, decreasing the relative amount of $C_6H_{11}OOH$ may indicate partial elimination of the free radical steps from the overall process mechanism.[18] The putative steps of the consecutive transformation of cyclohexylhydroperoxo radical (C1) are depicted in Scheme 2 below. More rationales concerning the mechanism of the revealed features were reported earlier.[14]

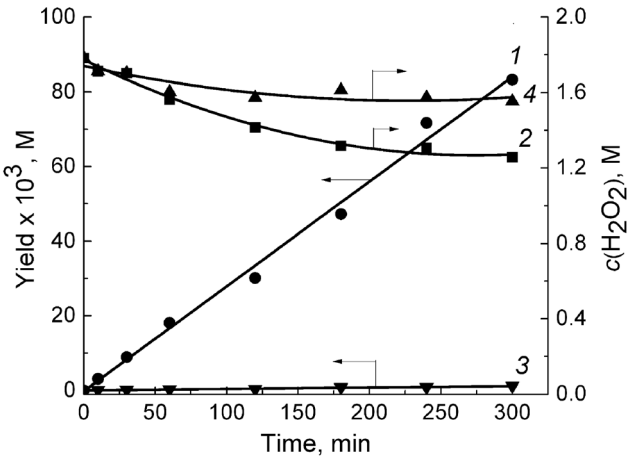

Fig. 1 The kinetics of product accumulation (1, 3) and H_2O_2 consumption (2, 4) without (3, 4) and with 25 mM (1, 2) of OxalH. Oxidation conditions: $C_6H_{12} = H_2O_2 = 1.8$ M, $VO(acac)_2 = 0.05$ mM, 40 °C, 5 h, MeCN.

In order to evaluate the impact of cation nature, C_6H_{12} oxidation was also carried out in the presence of $Co(acac)_2$ (Table 1, entries 9–11). For this catalyst, whether oxalic acid was present in the initial reaction solution or not, the set of products (COL, CON, and CHHP) remained the same as in case of $VO(acac)_2$. Nevertheless, the total yield was strictly dependent on the catalyst cation nature. For example, while oxalic acid additives clearly enhance the productivity of $VO(acac)_2$-based process, the mixing of OxalH with $Co(acac)_2$ was highly detrimental for the yield (compare entry 4 with 10 and 9 with 10, 11, Table 1). The revealed disparity in the action of oxalic acid was addressed to the noteworthy differences in the solubility of the respective oxalate salts. The reason is that right after supplementing the $Co(acac)_2$ solution with OxalH, the resultant mixture becomes opaque and a fine salmon powder, presumably Co(II) oxalate dihydrate,[19] starts to precipitate. Instead, the light-blue solution of $VO(acac)_2 + H_2C_2O_4$ remains transparent for weeks. Owing to the insolubility of Co-oxalate salt, one can expect that the lack of Co^{2+} ions in the reaction solution brings the overall process down. In the case of $Co(acac)_2$, already

$$H_2O_2 + V^{+4}O^{1+2} + 0.5O_2 \rightarrow V^{+5}O_2^{1+} + HO^{\bullet} + HO^{-} \quad (1a)$$

$$H_2O_2 + V^{+5}O_2^{1+} \rightarrow V^{+4}O^{1+2} + HO_2^{\bullet} + H^+ + 0.5O_2 \quad (1b)$$

$$H_2O_2 + V^{+4}O(C_2O_4)_2^{1-2} + 0.5O_2 \rightarrow V^{+5}O(\eta^2\text{-}O_2)(C_2O_4)^{1-} + {}^{\bullet}C(O)OH + CO_2 + HO^- \quad (1c)$$

$$H_2O_2 + V^{+4}O(C_2O_4)_2^{1-2} + H^+ \rightarrow VO(O)(C_2O_4)^{1-} + {}^{\bullet}C(O)OH + CO_2 + H_2O \quad (1d)$$

$$H_2C_2O_4 + HO^{\bullet} \rightarrow CO_2 + H_2O + {}^{\bullet}C(O)OH \quad (2a)$$

$$H_2O_2 + HO^{\bullet} \rightarrow H_2O + HO_2^{\bullet} \quad (2b)$$

$$H_2O_2 + V^{+4}O^{1+2} + H^+ \rightarrow V^{+5}O_2^{1+} + H_2O \quad (3a)$$

$$H_2O_2 + 2H^+ + 2e^- \rightarrow 2H_2O \quad (3b)$$

$$V^{+4}O^{1+2} + HO^{\bullet} \rightarrow V^{+5}O_2^{1+} + HO^- \quad (4a)$$

$$V^{+5}O_2^{1+} + HO_2^{\bullet} \rightarrow V^{+4}O^{1+2} + O_2 + H^+ \quad (4b)$$

$$V^{+5}O_2^{1+} + {}^{\bullet}C(O)OH + H^+ \rightarrow V^{+4}O^{1+2} + H_2O + CO_2 \quad (4d)$$

Scheme 1 The key initial stages in H_2O_2 decay assisted by $VO(acac)_2$ and $VO(acac)_2$ + OxalH: initiation (1), propagation/degenerative branching (2), heterolytic cleavage (3), and termination (4), respectively. The steps involving the participation of radicals originating from the CHHP homolysis are omitted for the sake of simplicity (mechanism of CHHP decay induced by radicals is given in Scheme 2 and reported earlier).[14] Steps (1a) and (1b) display the Haber–Weiss cycle.[21]

minimal (1 mM) content of oxalic acid was disadvantageous with respect to the product yield, even when comparing with the one obtained in the acid-free process (run 9, 11). The value of COL/CON/CHHP distribution in acid-free Co-catalyzed oxidation (1/2/97) was rather different than that obtained from $VO(acac)_2$ (6/12/1) (compare run 9 with 2, Table 1). In addition, these ratios differ from the COL/CON proportion (2/1) reported by Emanuel and coauthors for the Co-based process.[20] The explanation of such a discrepancy is as follows: (i) the lack, at that time, of proper techniques to simultaneously distinguish between the true content of COL and CON in the mixture with CHHP (this drawback was solved much later by elaboration of the triphenylphosfine method);[18] (ii) we use H_2O_2 as the oxidant and carry out the oxidation in MeCN solution, whereas the authors[20] report the results obtained by O_2-piloted oxidation carried out in bulk.

It is puzzling but apart from a very few examples,[14,17] the process efficacy estimation was based on exclusively investigating the yield, conversion, and selectivity. On the other hand, establishing the effectiveness of oxidant (H_2O_2) consumption ($Eff_{H_2O_2}$ – a quotient between the moles of H_2O_2 decayed/moles of products formed) would provide us with valuable information related to both the process efficacy and mechanism. Such curiosity motivated us to fill up this lack of knowledge in the hope that such data would be meaningful for the attainment of optimal process conditions. As is apparent, the $Eff_{H_2O_2}$ value was strongly dependent on OxalH, starting from a very tiny amount of the latter (Table 1, entry 2 and 3). In order to double the discussed parameter, the OxalH/$VO(acac)_2$ ratio should be kept above 10 (Table 1, entry 3 and 4). Further, the multiplication of OxalH content by three (run 5) or even by thirty (run 6) times led to a rather moderate (1.3 ÷ 1.5 times) increase in the $Eff_{H_2O_2}$ (Table 1). The best result was obtained when the mixture consisted of very low (0.06 mM) $VO(acac)_2$ content and the OxalH/$VO(acac)_2$ ratio was slightly below 1000 (run 7, Table 1). In this case, the calculated $Eff_{H_2O_2}$ value (about 42%) was close to the stoichiometric amount of oxygen that can be released in the course of H_2O_2 decomposition (50%). The last results correspond to the yield dependencies and supplement our early speculation about the role of OxalH in diminishing the free radical counterpart of H_2O_2 decay. The reason is that homolytic cleavage of peroxides led to the generation of free radicals. The last ones can further induce extra decay of H_2O_2 and, in turn, increase the unproductive consumption of the latter. On the contrary, in the presence of OxalH, this kind of H_2O_2 decomposition can be hampered to a large degree by shifting the mechanism to the non-radical domain.[14] As a consequence, the overall process effectiveness increased due to both higher conversion and selectivity. The lowering of initial content of CyH from 1.8 M to 0.18 M improved the cyclohexane conversion by roughly six times (from approx. 5%, entry 4 to 30%, entry 8). Nevertheless, in the last case, the $Eff_{H_2O_2}$ value decreased by 2.5 times, probably because of lower load of OxalH (compare entry 7 and 8, Table 1).

3.1.2 Relationship between the reaction mixture conductance and process yield. According to the Table 1 and Fig. 2 and 3, the highest yield of the desired products was obtained in the mixtures composed of 0.20–0.25 mM of $VO(acac)_2$ and 20–30 mM of OxalH. For values below or above these indicated intervals, the process productivity was found to be lower regardless of alteration of $VO(acac)_2$ (Fig. 2) or OxalH (Fig. 3) constituents. It is well known that metal cations of the catalyst are involved in the radical steps of the process mechanism, namely, initiation, degenerative branching, propagation, and termination (Schemes 1 and 2). Nevertheless, such contribution may not be limited by such participation only. The reason is that the ions originating from dissociation of

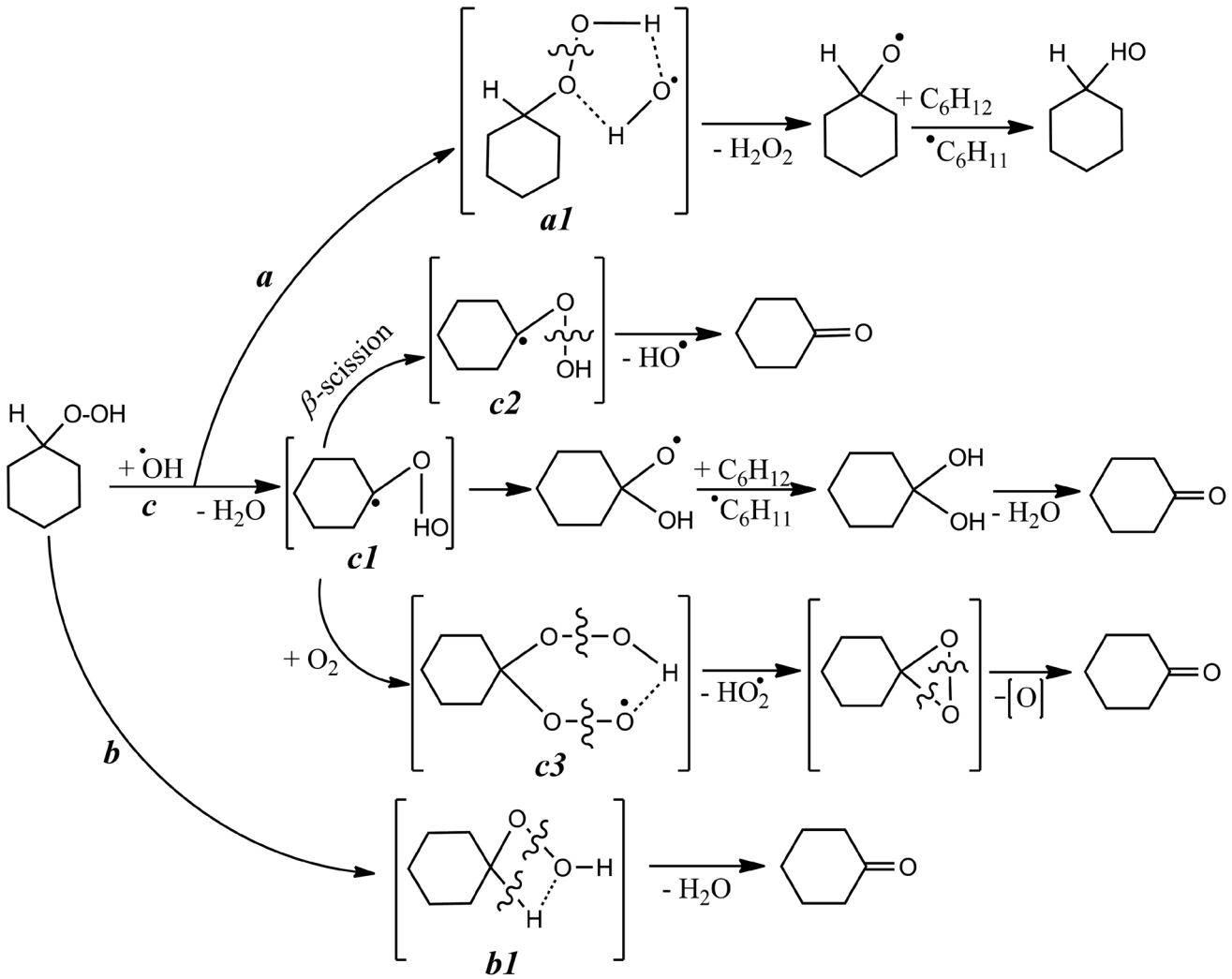

Scheme 2 Key putative stages of radical-induced CHHP decay. For sake of clarity, the bond dissociation energy (BDE) values of –O–O– in CHHP, C–H and –OO–H were taken equal 40, 93 and 86 kcal mol^{-1}, respectively.[22,23]

the metal-based catalysts can modify the electrochemical properties of the reaction medium. This feature of soluble metallocomplexes, along with their participation in the set of elemental reactions, altogether may affect the yield and product distribution. To date, there are very few publications that have focused on studying the impact of the reaction mixture composition on the process electrochemistry. In addition, they mainly reported the current–voltage dependencies.[24] Similarly, the kinetics of the process were scrutinized considering the electrochemical parameters but again in relation with the pure solvents only.[16] Furthermore, there were no data (except the revealed relationships between the yield and reaction medium relative dielectric permittivity)[17] that bring together the process efficacy and electrical conductance of the real reaction mixture. The study undertaken for yield *vs.* $1/G$ gave the results presented below.

The decrease in the solution $1/G$ value caused by $VO(acac)_2$ addition indicates that the revealed effect may be stipulated by the ions originating in the course of metal salt dissociation. The profile of $1/G$ *vs.* $VO(acac)_2$ shows a rapid decrease till 0.20 mM concentration of the metallocomplex, followed by saturation of the investigated parameter value when its content exceeded this level (Fig. 2, inset, curve 3). The slope of this curve shows the initial drop of 350 kOhm M^{-1}. Such a trait indicates that $VO(acac)_2$ is a weak electrolyte.[25] Exceeding the 0.20 mM concentration of $VO(acac)_2$ in the solution does not lead to further elevation of ion concentration caused by the attainment of the dissociation/association equilibrium. In other words, at the studied experimental conditions, the concentration of the ions (VO^{2+} and $acac^{-1}$) does not surpass 0.20 mM, regardless of the total content of the metal salts. Hence, simply increasing the content of $VO(acac)_2$ is not enough to lessen the $1/G$ value. The mirror-shaped symmetry between $1/G$ and the yield dependence maintained within the entire interval of $VO(acac)_2$ concentrations (curves 1 and 3) corresponds well with this assumption.

The addition of oxalic acid into $VO(acac)_2$ solution dramatically reduces the $1/G$ value from 80 kOhm to 18 kOhm (Fig. 2, inset). By contrast, the initial slopes of $1/G$ *vs.* $VO(acac)_2$

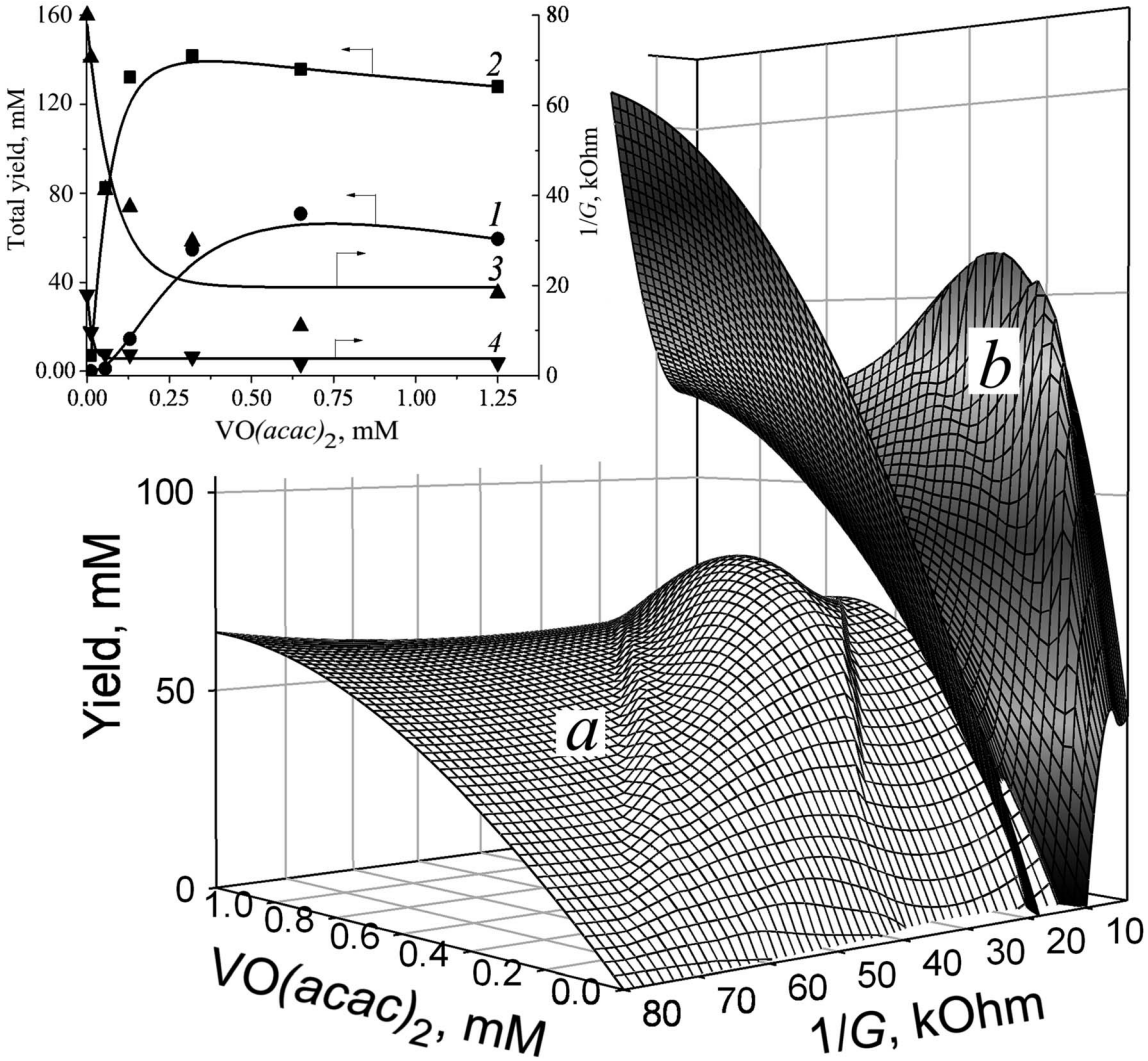

Fig. 2 The relationships between total yield, reaction medium $1/G$ value, and $VO(acac)_2$ content. (a) in the absence; (b) in the presence of 15 mM of OxalH. Inset: yield (1, 2) and $1/G$ (3, 4) dependence taken in the absence (1, 3) and presence (2, 4) of OxalH. Oxidation conditions: CyH = H_2O_2 = 1.8 M, 40 °C, 5 h, MeCN.

dependence for $VO(acac)_2$ and $VO(acac)_2$ + OxalH compositions remain almost intact and are equal 3to 50 kOhm mM^{-1} (curve 3) and 330 kOhm mM^{-1} (curve 4), respectively. In spite of that, the presence of OxalH causes the narrowing of the concentration interval of $VO(acac)_2$ (from 0.125 ÷ 0.25 mM, curve 3 to 0.04 ÷ 0.05 mM, curve 4) within which the change in $1/G$ is completed. Surprisingly, the ratio of the initial/final $1/G$ values significantly increased from ~4 for $VO(acac)_2$ solution (the initial and final $1/G$ level is equal to 80 kOhm and 19 kOhm, respectively, curve 3) to ≈16 for the $VO(acac)_2$ + OxalH mixture (80 kOhm and 5 kOhm, respectively, curve 4). The rationale of the revealed trait is the dominance of the reverse process (association) whenever $VO(acac)_2$ or OxalH concentration exceeds the predetermined concentration.

The stepwise supplementation of the $VO(acac)_2$ solution with OxalH affects both the $1/G$ and yield values (Fig. 2 and 3). The 3D image (Fig. 3, curve in red) indicates that this effect has, in fact, a multifactorial nature. In the beginning, up to 40 mM content, the OxalH additives afford consistent and noticeable increase in the yield. Simultaneously, with the increase in the yield, the increase in $1/G$ also altered but in the opposite manner, as described by the projection of the red curve on the *XY* plane (left wing of the blue curve, Fig. 3). Further, steadily increasing the OxalH concentration worsened the solution conductance (right wing of the blue curve) and deteriorated the yield (red curve obtained when OxalH content exceeds 40 mM). Eventually, the reason of the last peculiarity can be the competition among the dissociation/association steps similarly when $VO(acac)_2$ is taken solely (Fig. 2 and related discussion above). Such a process may also be responsible for the revealed reduction in the conductance and associate it with the retardation of oxidation at high content of OxalH (Fig. 3). The decrease in the oxidation efficiency caused by an excess of OxalH can be attributed to the acceleration of heterolytic cleavage of H_2O_2 at very low pH (more details concerning issue are given below in Section 3.2).[17]

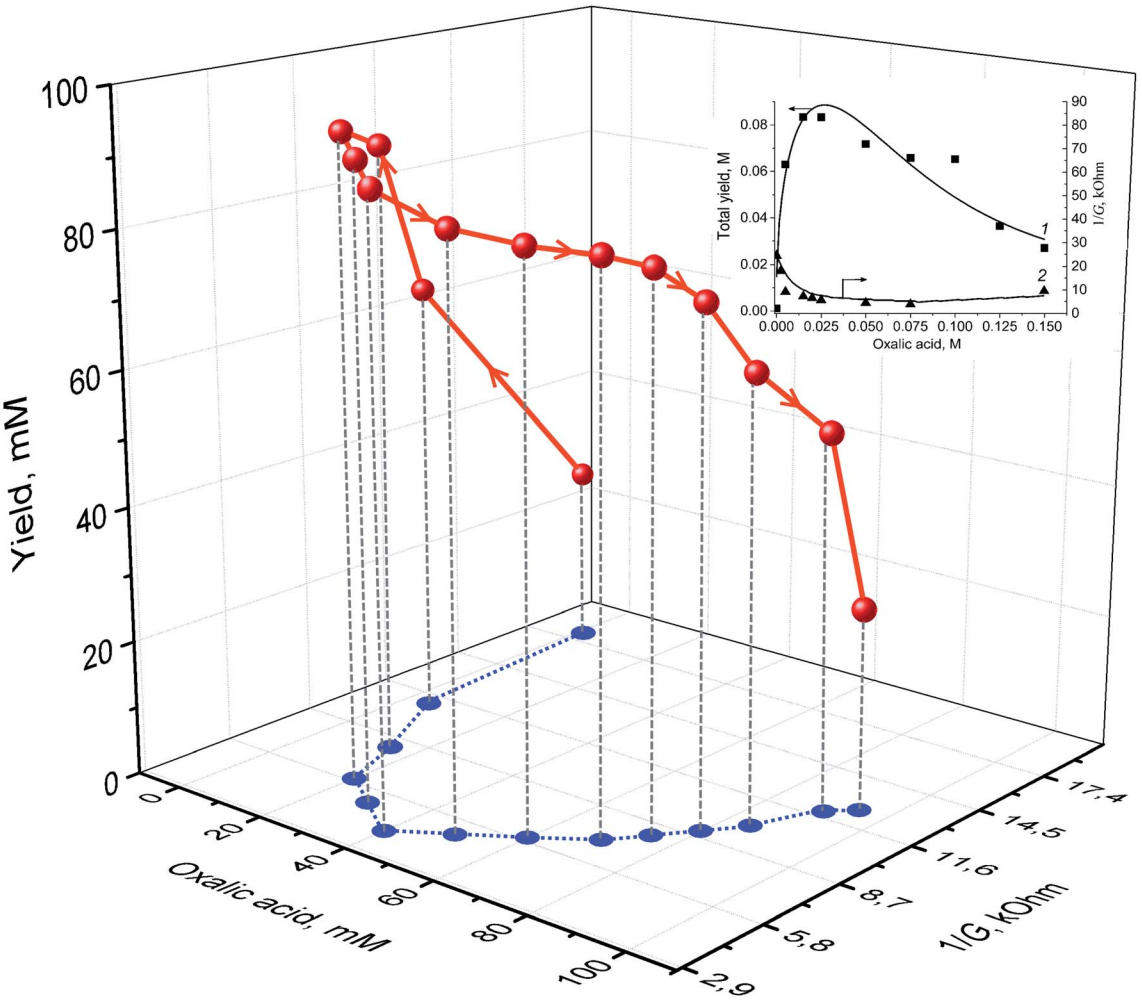

Fig. 3 The relationships between OxalH concentration, reaction medium 1/*G* value, and product yield. Inset: yield (1) and 1/*G* (2) *vs.* oxalic acid dependence. Starting reaction conditions: $C_6H_{12} = H_2O_2 = 1.8$ M, 0.125 mM of $VO(acac)_2$, 40 °C, 5 h, MeCN.

The concentration range of OxalH in $VO(acac)_2$ + OxalH mixture at which the trends of both the yield and 1/*G* *vs.* OxalH dependence changed to the opposite ones was ~20–40 mM (Fig. 3). The last value is about 50–100 times (20 mM/0.2 mM = 100) higher compared to that displayed by the $VO(acac)_2$ solution (~0.20 mM) (Fig. 2, inset, curve 3) and is accompanied by a conspicuous (more than four times, 90 mM/20 mM = 4.5) enhancement in the product yield (Fig. 2 and 3). Hence, one can assume that dissolving OxalH affords much more charged species that are responsible for higher conductance and presumably increases the yield as well. Again, the 4-times lower minimal value of 1/*G* was registered for the $VO(acac)_2$ + OxalH system (~5 kOhm, Fig. 3 and inset) compared to the minimal level of 1/*G* of about ~20 kOhm intrinsic to the $VO(acac)_2$ solution (Fig. 2, inset, curve 3). We explain the revealed deviation by the smooth dissociation of oxalic acid ($pK_a^{aqua} = 1.27$) in MeCN[26] due to the similarity of the donor number of this solvent (14.1 kcal mol^{-1}) and water (18 kcal mol^{-1}).[27] Given that the increased conductance of the systems constituted with $VO(acac)_2$ + OxalH can be subjected to protons and, although to a lesser degree, anions. The reason is that the former species are incomparably smaller ($r = 0.877$ fm)[27,28] than VO^{2+} ($r = 158\,933$ fm, this study) and thus, are much more mobile, bear higher charge density, and can transport a charge superior to that transported by bulky metal ions (see the paragraph below).

Apart from the conductance afforded by the charged species, the increase in the conductance in aprotic polar (*i.e.*, MeCN) medium may occur *via* "hop-turn" mechanism, which was first suggested by Grotthuss and then by Nagle.[29,30] Due to such a scenario, the formation of hydrogen bonds may occur between oxalic acid and its conjugate base $HC_2O_4^-$ or $C_2O_4^{2-}$ (homo-conjugation, Scheme 3). As a consequence, it can boost the acidity of the solution and reduce the pK_a by stabilizing the conjugate base and increasing the proton-donating power of the acid.[30] Such a feature may prevent the self-oligomerization of OxalH at low concentration (contrary to well-known acetic acid dimer formation) and therefore, favors the protons (*i.e.*, charge) transfer. It can be predict qualitatively that the conductivity (or mobility of H^+) should decrease as the concentration of OxalH increases (similar to the event when HCl is dissolved in water).[31] Then, the association of $H_2C_2O_4$ molecules as well as the reverse proton-anion coupling explains the reduction in the 1/*G* level

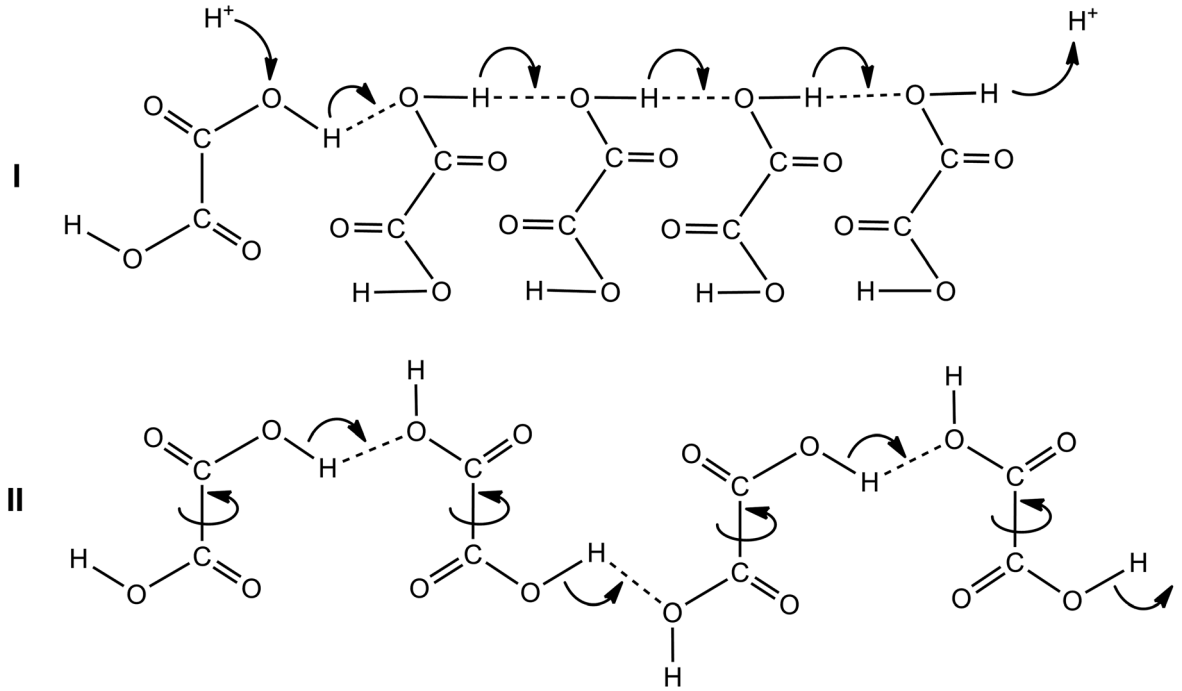

Scheme 3 The putative "hop (I)-turn (II)" mechanism of conductance afforded by the protons of oxalic acid in polar aprotic solvent.

and corresponds to the total and CHHP yield alteration (Table 1, Fig. 3, Scheme 2). Similarly, such a feature may be responsible for preventing the decrease in the pH level when the concentration of OxalH exceeded its predetermined concentration in the reaction mixture (Fig. 4 below).

Together, the above results demonstrate the role that electric conductance may play in the chemical process. However, besides G, there could be additional electrochemical parameters responsible for the effectiveness of the studied system, which were not defined herein. For example, the decrease in $1/G$ may be accompanied with the alteration in the acidity level, thus leading to a reduction in the self-decay of, for *e.g.*, active metal-peroxo $VO(\eta^2\text{-}O_2)(oxal)^-$ species, which is beneficial for the yield.[17] The forthcoming section evaluates the expressed assumptions.

3.2 Study of the influence of oxalic acid on the pH/redox potential of the reaction medium

In order to gain more insight into the electrochemical factors that affect CyH oxidation along with $1/G$, the pH/redox potential (ORP) studies were undertaken. The kinetic profiles of pH and $1/G$ likewise showed a decrease for the $VO(acac)_2$ (steeper) or $VO(acac)_2$ + OxalH (slight) solutions right after they were mixed with H_2O_2 (Fig. 4). Inset (a) of this figure represents a plain line with the slope of "5.93", which was plotted by subtraction of the pH level of $VO(acac)_2$ solutions containing the different additives of OxalH from the pH value of initial $VO(acac)_2$ solution (the last one was equal to 6.92). The dashed line with the slope of "0.56" shows the alteration in the pH of the $VO(acac)_2$ + OxalH mixture in the presence of H_2O_2. The dotted line with the slope of "−5.23" was plotted using the differences between the pH of the $VO(acac)_2$ + OxalH solutions and acidity levels obtained once H_2O_2 was injected. The digits next to the experimental points correspond to the numbers marking the respective curves in the main plot. Inset (b) shows a straight line (slope "0.28"), which demonstrates the E_h *vs.* OxalH dependence in the respective $VO(acac)_2$ + OxalH solutions. The dashed line (slope "−0.03") shows the E_h *vs.* OxalH dependence once H_2O_2 is added. The dotted line (slope "−0.31") was obtained by subtraction of the E_h data of the solid line (slope "0.28") from the respective E_h represented by the dashed line (slope "−0.03"). The E_h values were calculated using eqn (II) below. The digits next to the experimental points in both the insets correspond to the ones marking the respective curves in the main graph.

The most conspicuous impact on pH (about 9.3 units, from 6.92 to −2.40) is demonstrated by the addition of H_2O_2 into the solutions containing solely $VO(acac)_2$ (curve 1, Fig. 4). Considering that the pH in the concentration range of 2.9–26.5 M of H_2O_2 equals 4.9–5.3,[32] it was impressive to detect such an evident deviation from the actual concentration of H_2O_2 (7.5 mM) from the tabulated data. Since H_2O_2 and $VO(acac)_2 + H_2O_2$ solutions differ from each other by $VO(acac)_2$ only, one can suppose that the latter component was responsible for the revealed trait. Such a dramatic pH decrease evidently results from the presence of some sort of product formed in the course of $VO(acac)_2 + H_2O_2$ interaction. The species that are most probably liable for the detected abnormality are radicals (particularly hydroxyl ones) generated by the catalytic homolysis of H_2O_2 (Scheme 1). Such species are exceptionally strong oxidizers with average rate constants of H-atom abstraction in the range of 10^8 to 10^9 M^{-1} s^{-1}.[33] On the other hand, they possess an extremely acidic nature, reflected by very high

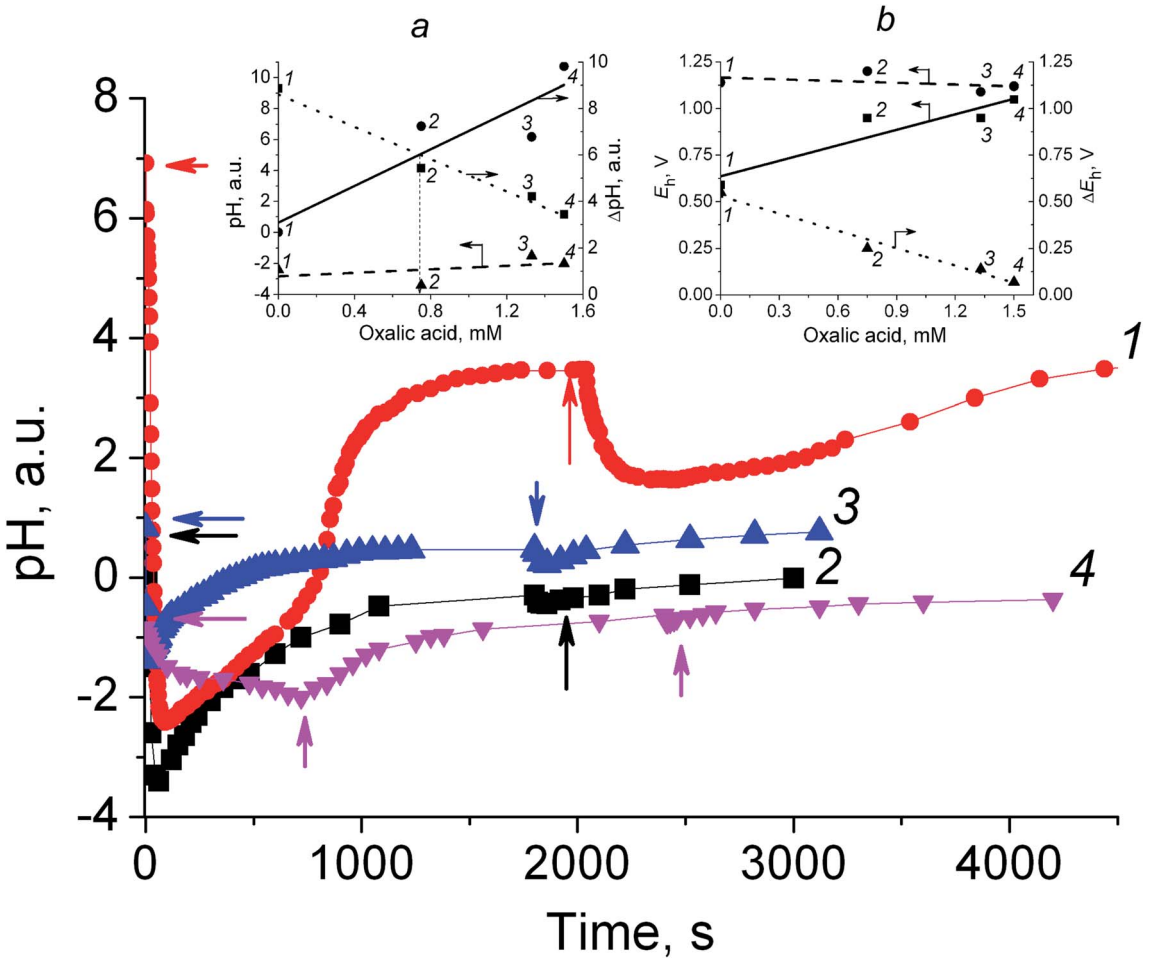

Fig. 4 Time-trace of pH taken after the addition 2 μL of 35% H_2O_2 (corresponds to 7.5 mM of hydroperoxide in the reaction solution). The initial reaction mixtures comprise 0.75 mM $VO(acac)_2$ (1); 0.75 mM $VO(acac)_2$ + 0.75 mM OxalH (2); 3.0 mM $VO(acac)_2$ + 1.4 mM OxalH (3); 0.75 mM $VO(acac)_2$ + 1.5 mM OxalH (4) in 8 mL MeCN, 20 °C. The arrows mark the time at which H_2O_2 was injected. Insets: the pH (a) and E_h (b) *vs.* OxalH dependence (plain lines) and the impact of H_2O_2 on these parameters (dashed and dotted lines). (a) Plain line was plotted by the subtraction of the pH of $VO(acac)_2$ + OxalH solutions from the pH value of initial $VO(acac)_2$ solution (the last one was equal to 6.92); the dashed line depicts the pH of $VO(acac)_2$ + OxalH alteration caused by H_2O_2 addition; the dotted line depicts the values obtained by the subtraction of the pH of $VO(acac)_2$ + OxalH solutions from the pH level obtained once H_2O_2 was injected; (b) plain line demonstrates the E_h *vs.* OxalH dependence in the respective $VO(acac)_2$ + OxalH solutions; the dashed line depicts the E_h *vs.* OxalH dependence once H_2O_2 was added; the dotted line was obtained by the subtraction of the E_h data of the solid line from the respective E_h value depicted by the dashed line. The E_h values were calculated using eqn (II).

reduction potential of 1.8–2.7 V (depending on the pH).[34] Oxalic acid taken even in small concentrations minimizes the impact of H_2O_2 on the pH of $VO(acac)_2$ solution; the acidity level before and after H_2O_2 addition differs by 1–4 units only (compare curve 1 with 2–4, Fig. 4). The dashed line with the tiny slope of 0.56 illustrates the negligible response of the pH of $VO(acac)_2$ + OxalH mixture on the H_2O_2 additive (inset (a), Fig. 4).

Besides this, complementing the $VO(acac)_2$ + OxalH solution with H_2O_2 results in the linear dependence of pH *vs.* OxalH (inset (a), slope equal 5.93) compared to the one (−5.23) obtained for $VO(acac)_2$ + H_2O_2. The ability of H_2O_2 to affect the pH steadily diminished once the content of oxalic acid increased (curves 2, 3, 4 in the main figure; dashed line with slope 0.56 in the inset). Then, one can admit that the role of the species originating from H_2O_2 decomposition (predominantly highly acidic HO˙ radicals) in the pH alteration is reduced. In other words, as long as the acidity of the initial $VO(acac)_2$ + OxalH solution increased (Fig. S2†), it loses the susceptibility to further H_2O_2 additions (Fig. 4). Such a trait may reflect that the heterolytic decay starts to prevail over the homolytic one (*i.e.*, the income from reactions (1c), (1d), and (3) of Scheme 1 is diminished).[35] Otherwise, H_2O_2 additives would have similar effects on both $VO(acac)_2$ and $VO(acac)_2$ + OxalH pH profiles (Fig. 4, curve 1 and 2–4, respectively).

Interestingly, the line that depicts the pH of $VO(acac)_2$ + H_2O_2 *vs.* OxalH dependence (dashed line with the slope of 0.56) does not cross the solid line ($VO(acac)_2$ + H_2O_2) – 6.92 *vs.* OxalH (slope 5.93) (6.92 is the pH of the $VO(acac)_2$ solution). On the other hand, the last line and the dotted one obtained by subtraction of the pH of $VO(acac)_2$ + OxalH solutions from the pH of $VO(acac)_2$ + OxalH + H_2O_2 (line with slope of −5.23) cross each other at OxalH content *ca.* 0.8 mM (Fig. 4, inset (a)). The

detected progressive decline in the relative differences in the acidity level (ΔpH, dotted line, inset (a)) correlate with the elevation in OxalH content and may reflect the decrease in HO$^{\bullet}$ radical generation, thus showing that heterolytic H_2O_2 cleavage prevails over the homolytic one. The last peculiarity may also be responsible for the revealed disadvantage of both oxidation productivity and the yield of CHHP attained at high content of OxalH.

The extrapolation of the dotted line in inset (a) (Fig. 4) would result in it crossing the *X*-axis at the point *ca.* 2.5 mM of oxalic acid content, indicating that extra OxalH additives may not decrease the acidity any more. On the other hand, the most effective (*i.e.*, affords the highest yield) concentration of OxalH in the oxidizing mixture was 20–30 mM, which is roughly 10 times higher than this value (Fig. 3). With such a feature, we conclude that the proton-induced conductance has a privilege at small concentration of OxalH whereas the molecular moiety (realized *via* "hop-turn" mechanism) prevails at higher concentration. Again, when the content of OxalH exceeds the predetermined level of 30–40 mM, the processes of ions association as well as oligomerization of non-dissociated molecules of OxalH (section above) become prevalent, thus hampering the *G* and, as a result, the yield as well.

The alteration of pH also affects the redox potential. If so, the acidity level and redox potential may relate to each other in the manner of E_h − pH, where E_h is the cell potential. In case of pH-dependent potential, the equation depicts that it should involve either H^+ or HO^- ions (reaction (3), Scheme 1). The investigated systems reveal such a trait. Regarding the reactions (mainly the steps reflecting VO^{2+} oxidation to VO_2^+), they are one-electron reactions and are characterized by the oxidized and reduced species of one kind only. In addition, the redox reactions are carried out in dilute solutions at 25 °C. Based on the above issues, for the calculation of E_h dependence of H^+ concentration, the Nernst equation was expressed in terms of concentration:

$$E = E^0_{redox} - 0.0592 \log_{10} Q = E^0_{redox} - 0.0592 \log_{10}[Ox]^a/[Red]^b[H^+]^m \quad (I)$$

where E – redox potential; E^0_{redox} – standard (formal) redox potential (assuming standard conditions for the actual acidity of the solution) for VO^{2+}/VO_2^+ pair in acetonitrile is equal to +1.00 V. The value of this potential can be taken as the average of voltammetric maximum peak potentials $(E_{p,ox} + E_{p,red})/2$ from the cyclic voltammetry experiments.[36] For our particular case, $E_{p,VO(V)}$ and $E_{p,VO(IV)}$ values in MeCN were equal to 0.98 V and 0.92 V, respectively (see Chapter 3.3); Q – the reaction quotient; [Ox]/[Red] – the ratio of oxidized and reduced form; a, b, m – stoichiometric coefficients; $[H^+]$ – concentration of hydrogen ions.[37]

For the sake of practical usage, eqn (I) was written in the abridged mode (II), which connects together pH and redox potential as:

$$E_h = E^0_{redox} - 0.0592\ pH \quad (II)$$

The slope (0.0585 V) of the straight line for the redox potential (ORP) *vs.* pH plot (Fig. S3†) matches well with the *RT*/*Fn* coefficient of Nernst equation (0.0592 V). The last peculiarity may indicate that to a first approximation, the eqn (II) can be used for adequately describing our experimental results. The insets (a) and (b) of Fig. 4 depict the similar tendencies of both pH and *E* parameters of $VO(acac)_2$-based solutions (compare the same type of lines – solid–solid, dash–dash, dot–dot in the insets (a) and (b)). For instance, the pH and *E* level values were not sensitive to H_2O_2 addition in the presence of OxalH (compare the dashed line in inset (a) with the dashed line in inset (b)). Similarly, the relative values of solution acidity alteration, ΔpH (dotted line, inset (a)) and redox potential Δ*E* (dotted line, inset (b)) after H_2O_2 addition were minimized by OxalH additive. In addition, both these characteristics gradually decreased once the oxalic acid concentration in $VO(acac)_2$-based mixture was raised.

As the redox reaction proceeds, the cell potential gradually reduced until the reaction attained equilibrium, at which change of Gibbs free energy $\Delta G = 0$. Given this, the reaction quotient $Q = K_{eq}$ and $\Delta G = -FE$, so $E = 0$. Then, $0 = E^0 - 0.0592/\log_{10} K_{eq}$ and $\log_{10} K_{eq} = E_0/0.0592$. In our case, $E_0 = 1.00$ V ($VO^{2+} \rightarrow VO_2^+$ process), $\log_{10} K_{eq} = 1.00/0.0592 \times 1 = 16.9$ and $K_{eq} = 1016.9$. Because $K > 1$ and $E0 > 0$, the equilibrium of the above reaction should be shifted to the right side. Visually, it is reflected by the almost instant replacement of the blue color of the initial VO^{2+} solution ($\lambda_{max} \approx 400$ nm) by the yellow color of the VO_2^+ species ($\lambda_{max} = 460$ nm) once H_2O_2 was added.[14]

3.3 Impact of oxalic acid on the current–potential dependence

According to our previous study, the action of OxalH in $VO(acac)_2$-based solutions consists of reducing the pathways leading to the homolytic cleavage of H_2O_2 (*e.g.*, induced by free radicals). In turn, it resulted in the partial decrease in the role of free radicals in the process mechanism.[14,17] On the other hand, $1/G$ as well as alteration in the pH and E_h levels may affect the reaction mixture electric current *vs.* potential relationships as well. Should it happen, the *I vs. E* dependence can be registered by the CV technique. The results of such a viewpoint are discussed below.

The forward anodic scan of the initially light-blue solution of $VO(acac)_2$ (Fig. 5, curve 1) exhibits the oxidation peak at 0.98 V which, in fact, is coupled with a very weak reduction one that emerges at 0.92 V (reverse scan). In the second (cathodic) scan, one can observe the additional reduction peak with the maxima at −1.75 V. The CV also exhibited three oxidation peaks appearing in the course of the anodic scan at −1.60 V (which actually is quasi-reversible to the signal at −1.75 V of the previous scan), at −1.45 V (Fig. 5, curve 1), as well as the low and broad hill at −0.6 V. The reduction peak at −1.75 V was detected during the first cathodic scan (Fig. 5, inset). The second scan of this voltammogram shows oxidation peaks at −1.5 V and 1.00 V as well. On carrying out the last scan, a broad and low reduction signal with a maximum near 0.92 V was obtained. The quasi-reversible couple at 0.98 V/0.92 V, according to the data reported for similar systems by Kitamura and Reichel, may be

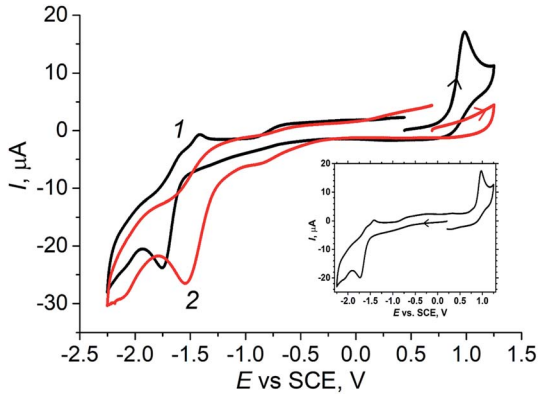

Fig. 5 CV diagrams of 1.25 mM $VO(acac)_2$ (1) and 1.25 mM of $VO(acac)_2$ + 2.5 mM of OxalH (2), MeCN, 20 °C, anodic scan. Inset: cathodic scan of the $VO(acac)_2$ solution.

a consequence of the reactions involving V^{+4}/V^{+5} transformation.[38] However, the height of the reduction peak is significantly lower than that of the oxidation one. The quasi-reversible signals emerging at −1.75 V/−1.60 V at the anodic and following cathodic scans (Fig. 5 and inset) can be assigned to the redox reactions of acac ligands.[39] Their intensity linearly decreased in the same way as displayed by the peak of VO^{2+} (0.98 V) and evidently occurs due to the gradual dilution of the original $VO(acac)_2$ solution (Fig. S4,† inset, line plotted by circles). The described behavior of such a system corresponds to the parallel attenuation of the peak at 0.98 V (Fig. S4,† inset, line plotted by squares), indicating that both the signals come from the same precursor.

The addition of oxalic acid to the solution of $VO(acac)_2$ noticeably modifies the CV (compare profiles of $VO(acac)_2$ and $VO(acac)_2$ + OxalH in Fig. 5). First of all, the peak at 0.98 V assigned to the oxidation of V(IV) was almost completely disappeared when $H_2C_2O_4$ concentration in the mixture becomes just two times that of $VO(acac)_2$ (Fig. 5, curve 2). Based on our previous results, we claim that it may be a consequence of the quick and complete substitution of acac ligands of $VO(acac)_2$ by oxalate ligands.[17] Instead, in the forward cathodic scan, a peak emerging at *ca.* −0.85 V in the presence of OxalH was registered. The gradual increase in the OxalH content in the $VO(acac)_2$ solution led to the emergence of one more signal at −1.55 V (Fig. 5 and S5†). On carrying out the CV of 2 mM of OxalH in MeCN, two reduction peaks appeared at the same positions of −0.85 V and −1.55 V (Fig. S6†). Then, one can assume that the last two peaks most probably reflect the redox reactions where oxalate anions participate. Interestingly, the slopes for acac (Fig. S4,† inset) and oxalate (Fig. S5,† inset) signals differ by about two times (−15.03/7.00 = 2.14). Supposedly, the reason for the revealed ratio may be two times as much (−2) charge on the latter ligand compare to that on the former (−1).

The addition of H_2O_2 to the initial solution of $VO(acac)_2$ dramatically increases the peak at −1.0 V (Fig. 6). Nevertheless, within 5 min, the intensity of this signal starts to lessen with almost the same rate (Fig. 6, inset (a)). On referring to a previous study,[17] it was found that such a signal may ensue from the

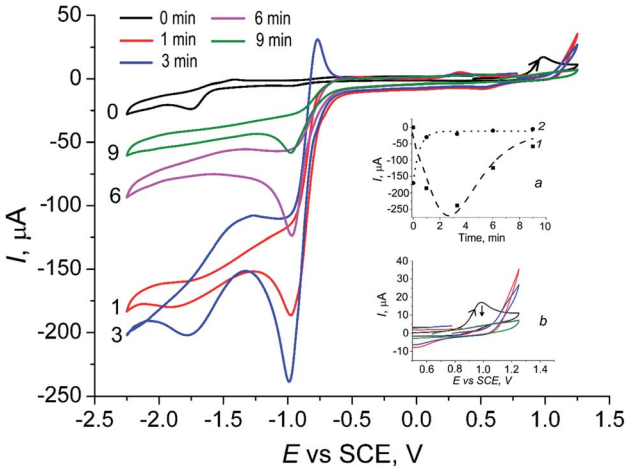

Fig. 6 CV of $VO(acac)_2$ solution taken after supplementing it with H_2O_2. The curves with various colors indicate the time at which the respective spectra were taken. Initial conditions: $VO(acac)_2$ (1.25 mM), 50 wt% aq. H_2O_2 (15 mM), MeCN, 20 °C. Insets: time-traces of the −1.0 V (1) and 0.98 V (2) peak height change, (a); the kinetics of V^{IV} signal vanishing, (b). The curves with various colors indicate the time at which the respective spectra were taken (the time order was the same as that in the main figure).

dioxygen released in the process of H_2O_2 decay. Furthermore, the mentioned reaction leads to a quick transformation of the parental V(IV) catalyst ions to the oxidized V(V) ions, which is substantiated by the almost instantaneous vanishing of the oxidation peak at 0.98 V (Fig. 6, inset (b)).

It is worth noting that the addition of H_2O_2 into the solution of $VO(acac)_2$ + OxalH causes certainly smaller (in comparison to oxalic acid-free process) changes in the height of the −1.0 V peak (compare Fig. 6 and 7). The last feature correlates with the behavior of pH envisaged in Section 3.2 above. The kinetics of the last signal height alteration exhibits clear relationships

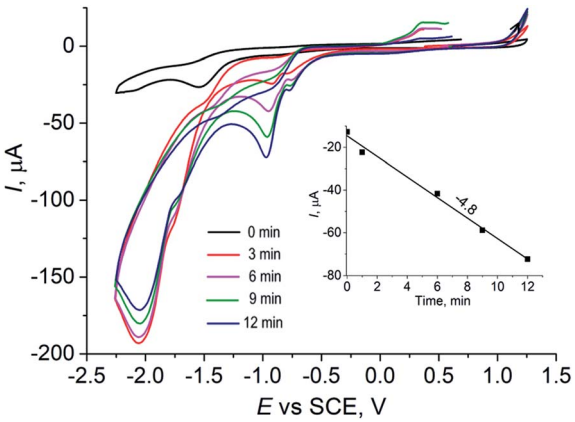

Fig. 7 CV of $VO(acac)_2$ + OxalH solution taken after supplementing it with H_2O_2. The curves with various colors indicate the time at which the respective spectra were taken. Initial conditions: $VO(acac)_2$ (1.2 mM), oxalic acid (2.5 mM), 50 wt% aq. H_2O_2 (15 mM), MeCN, 20 °C. Inset: time-trace of −1.0 V peak height changing. The curves with various colors indicate the time at which the respective spectra were taken (the time order was the same as that in the main figure).

between the presence of oxalic acid and the intensity of O_2 evolution. For example, in the case of OxalH-free experiments, the rapid increase in the dioxygen peak detected right after H_2O_2 injection was followed by its rapid decrease (Fig. 6, inset (a)). In contrast, in the presence of two equivalents of oxalic acid, the slope of the curves depict that the kinetics of O_2 signal change was leveled out by roughly 17 times ($\{0 - (-250)\}/3$ mA min^{-1}/4.8 mA $min^{-1} \sim 17$) (confer inset (a), curve 1 of Fig. 6 and 7). In addition, H_2O_2 did not affect the CV of $VO(acac)_2$ + OxalH mixture within the region near 0.98 V, where V(IV) oxidation was revealed (compare Fig. 5 and 7). Elucidation of the absence of the 0.98 V oxidation peak in the presence of OxalH is still under study.

4. Conclusion

This work has shown the noticeable impact of reaction medium electric conductance G (or *vice versa* resistance, $1/G$) on the yield of H_2O_2-piloted mild cyclohexane oxidation rendered by vanadyl(IV) acetylacetonate as the starting catalyst and oxalic acid as the promoter. The combination of impedance, pH, and CV techniques allowed to establish the impact of oxalic acid on $1/G$, pH/redox potential, and current–voltage dependencies. The decrease in solution $1/G$ in aprotic polar solvents may emerge on elevating the concentration of H^+, $HC_2O_4^-$, and $C_2O_4^{2-}$ as well as VO^{2+} and $acac^-$ ions' origin. The H-bonded networks created by $H_2C_2O_4$ molecules and realized through "hop-turn" mechanism favors the decrease in $1/G$ value. Surpassing the 30 mM of OxalH content leads to further change in $1/G$ but simultaneously worsens the yield. The prevalent heterolytic cleavage of both H_2O_2 and CHHP in highly acidic conditions may be responsible for the revealed threshold. Oxalic acid also affects the value, shape, and behaviour of electric current *vs.* potential dependencies. Such features indicate that the presence of species different than that prevailing in OxalH-free oxidation. Some of them, for *e.g.*, the putative intermediates constituted with $VO(\eta^2\text{-}O)_2$ metal core may be responsible for the selective non-radical substrate oxidation. However, such features may prolong the catalyst life-time by, for example, curbing the V(IV) → V(V) irreversible oxidative catalyst destruction.

In turn, the application of a similar protocol (small-molecule V-based catalyst, oxalic acid as promoter, and H_2O_2 as oxidant, tuned electrochemical parameters) may be beneficial for the oxidation of other organic substrates of industrial interest.

Conflicts of interest

There are no conflicts of interest.

Acknowledgements

The authors are thankful to the staff of Physical Chemistry Department (Rzeszow University of Technology) for technical support, guidance, and courtesy essential to complete this research. We are indebted to Prof Andrzej Sobkowiak (Rzeszow University of Technology) for commentaries and Dr Jacques Muzart (CNRS – Universite de Reims Champagne-Ardenne) for numerous correspondences as well as to Mrs Dariya Maksym (Dept. of Physical Chemistry Institute of Physical Organic Chemistry and Chemistry of Coal NAS of Ukraine) for the assistance in GLC and pH analysis.

References

1 Y.-R. Luo, *Comprehensive handbook of chemical bond energies*, 2007.
2 Y. Ishii, S. Sakaguchi and T. Iwahama, *Adv. Synth. Catal.*, 2001, **343**, 393–427.
3 J.-M. Brégeault, *Dalton Trans.*, 2003, 3289–3302.
4 T. Punniyamurthy, S. Velusamy and J. Iqbal, *Chem. Rev.*, 2005, **105**, 2329–2363.
5 Y. Hitomi, K. Arakawa, T. Funabiki and M. Kodera, *Angew. Chem., Int. Ed.*, 2012, **51**, 3448–3452.
6 S. Lentini, P. Galloni, I. Garcia-Bosch, M. Costas and V. Conte, *Inorg. Chim. Acta*, 2014, **410**, 60–64.
7 M. M. Abu-Omar, A. Loaiza and N. Hontzeas, *Chem. Rev.*, 2005, **105**, 2227–2252.
8 R. A. Sheldon, I. Arends and U. Hanefeld, *Green Chemistry and Catalysis*, Wiley-VCH, 2007.
9 G. Licini, V. Conte, A. Coletti, M. Mba and C. Zonta, *Coord. Chem. Rev.*, 2011, **255**, 2345–2357.
10 P. Saisaha, J. J. Dong, T. G. Meinds, J. W. de Boer, R. Hage, F. Mecozzi, J. B. Kasper and W. R. Browne, *ACS Catal.*, 2016, **6**, 3486–3495.
11 Ch. Miao, H. Zhao, Q. Zhao, Ch. Xia and W. Sun, *Catal. Sci. Technol.*, 2016, **6**, 1378–1383 and references cited therein.
12 A. Pokutsa, K. Yu, A. Zaborovskyi, D. Maksym, J. Muzart and A. Sobkowiak, *Appl. Catal., A*, 2010, **390**, 190–194.
13 D. Rinaldo, D. M. Philipp, S. J. Lippard and R. A. Friesner, *J. Am. Chem. Soc.*, 2007, **129**, 3135–3147.
14 A. Pokutsa, Y. Kubaj, A. Zaborovskyi, D. Maksym, T. Paczesniak, B. Mysliwiec, E. Bidzinska, J. Muzart and A. Sobkowiak, *Mol. Catal.*, 2017, **434**, 194–205.
15 M. C. Foti, S. Sortino and K. U. Ingold, *Chem.–Eur. J.*, 2005, **11**, 1942.
16 Ch. Reichardt, *Solvents and solvent effects in organic chemistry*, Wiley-VCH Weinheim, 3rd edn, 2003.
17 A. Pokutsa, O. Fliunt, Y. Kubaj, T. Paczesniak, P. Blonarz, R. Prystanskiy, J. Muzart, R. Makitra, A. Zaborovskyi and A. Sobkowiak, *J. Mol. Catal. A: Chem.*, 2011, **347**, 15–21.
18 M. V. Kirillova, Y. N. Kozlov, L. S. Shul'pina, O. Y. Lyakin, A. M. Kirillov, E. P. Talsi, A. J. L. Pombeiro and G. B. Shul'pin, *J. Catal.*, 2009, **268**, 26–38.
19 J. Bacsa, D. Eve and K. R. Dunbar, *Acta Crystallogr., Sect. C: Cryst. Struct. Commun.*, 2005, **61**, 58–60.
20 I. V. Berezin, E. T. Denisov and N. M. Emanuel, *The Oxidation of Cyclohexane*, Pergamon, 1966.
21 F. Haber and J. Weiss, *Naturwiss*, 1932, **51**, 948–950.
22 E. Denisov and T. Denisova, *Dissociation Energies of O—H Bonds of Phenols and Hydroperoxides, Application of Thermodynamics to Biological and Materials Science*, ed. M. Tadashi, InTech, 2011.

23 E. T. Denisov and T. G. Denisova, *Handbook of antioxidants: bond dissociation energies, rate constants, activation energies and enthalpies of reactions*, CRC Press, Boca Raton, 2nd edn, 2000.
24 J. England, J. O. Bigelow, K. M. Van Heuvelen, E. R. Farquhar, M. Martinho, K. K. Meier, J. R. Frisch, E. Munck and L. Que Jr, *Chem. Sci.*, 2014, **5**, 1204–1215.
25 B. A. Averill and P. Eldredge, *Principles of General Chemistry, v. 1.0*, Saylor Foundation, Washington, 2011.
26 A. Kutt and I. Leito, *J. Org. Chem.*, 2006, **71**, 2829–2838.
27 D. T. Sawyer and J. L. Roberts, *Experimental Electrochemistry for Chemists*, John Wiley & Sons, NY, 1974.
28 R. Pohl, A. Antognini, F. Nez, *et al.*, *Nature*, 2010, **466**, 213–216.
29 C. J. T. Grotthuss, *Ann. Chem.*, 1806, **58**, 54–73.
30 J. F. Nagle and H. J. Morowitz, *Proc. Natl. Acad. Sci. U. S. A.*, 1978, **75**, 298–302.
31 S. Cukierman, *Biochim. Biophys. Acta*, 2006, **1757**, 876–885.
32 http://www.h2o2.com/faqs/FaqDetail.aspx?fId=26.
33 W. P. Kwan and B. M. Voelker, *Environ. Sci. Technol.*, 2002, **36**, 1467–1476.
34 O. Augusto and S. Miyamoto, Chapter II: Oxygen radicals and related species, in *Principles of Free Radical Biomedicine*, K. Pantopoulos and H. M. Schipper, Nova Science Publishers, 2011, vol. 1.
35 W. T. Hess, Hydrogen peroxide, in *Kirk-Othmer Encyclopedia of Chemical Technology*, Wiley, New York, 4th edn, 1995, vol. 13, pp. 961–995.
36 G. Zotti, G. Sciavon, A. Berlin and G. Pagani, *Synth. Met.*, 1991, **40**, 299–307.
37 P. Atkins, and J. de Paula, *Physical Chemistry for the Life Sciences*, New York, W.H. Freeman and Company, 2006, pp. 214–222.
38 M. Kitamura, K. Yamashita and H. Imai, *Bull. Chem. Soc. Jpn.*, 1976, **49**, 97–100.
39 M.-A. Nawi and T. S. Reichel, *Inorg. Chem.*, 1981, **20**, 1974–1978.